

Observation of the decay $\Lambda_c^+ \rightarrow \Sigma^- \pi^+ \pi^+ \pi^0$

M. Ablikim¹, M. N. Achasov^{9,e}, S. Ahmed¹⁴, M. Albrecht⁴, A. Amoroso^{50A,50C}, F. F. An¹, Q. An^{47,a}, J. Z. Bai¹, O. Bakina²⁴, R. Baldini Ferroli^{20A}, Y. Ban³², D. W. Bennett¹⁹, J. V. Bennett⁵, N. Berger²³, M. Bertani^{20A}, D. Bettoni^{21A}, J. M. Bian⁴⁵, F. Bianchi^{50A,50C}, E. Boger^{24,c}, I. Boyko²⁴, R. A. Briere⁵, H. Cai⁵², X. Cai^{1,a}, O. Cakir^{42A}, A. Calcaterra^{20A}, G. F. Cao¹, S. A. Cetin^{42B}, J. Chai^{50C}, J. F. Chang^{1,a}, G. Chelkov^{24,c,d}, G. Chen¹, H. S. Chen¹, J. C. Chen¹, M. L. Chen^{1,a}, S. J. Chen³⁰, X. R. Chen²⁷, Y. B. Chen^{1,a}, X. K. Chu³², G. Cibinetto^{21A}, H. L. Dai^{1,a}, J. P. Dai^{35,j}, A. Dbeyssi¹⁴, D. Dedovich²⁴, Z. Y. Deng¹, A. Denig²³, I. Denysenko²⁴, M. Destefanis^{50A,50C}, F. De Mori^{50A,50C}, Y. Ding²⁸, C. Dong³¹, J. Dong^{1,a}, L. Y. Dong¹, M. Y. Dong^{1,a}, O. Dorjkhaidav²², Z. L. Dou³⁰, S. X. Du⁵⁴, P. F. Duan¹, J. Fang^{1,a}, S. S. Fang¹, X. Fang^{47,a}, Y. Fang¹, R. Farinelli^{21A,21B}, L. Fava^{50B,50C}, S. Fegan²³, F. Feldbauer²³, G. Felici^{20A}, C. Q. Feng^{47,a}, E. Fioravanti^{21A}, M. Fritsch^{14,23}, C. D. Fu¹, Q. Gao¹, X. L. Gao^{47,a}, Y. Gao⁴¹, Y. G. Gao⁶, Z. Gao^{47,a}, I. Garzia^{21A}, K. Goetzen¹⁰, L. Gong³¹, W. X. Gong^{1,a}, W. Gradl²³, M. Greco^{50A,50C}, M. H. Gu^{1,a}, S. Gu¹⁵, Y. T. Gu¹², A. Q. Guo¹, L. B. Guo²⁹, R. P. Guo¹, Y. P. Guo²³, Z. Haddadi²⁶, S. Han⁵², X. Q. Hao¹⁵, F. A. Harris⁴⁴, K. L. He¹, X. Q. He⁴⁶, F. H. Heinsius⁴, T. Held⁴, Y. K. Heng^{1,a}, T. Holtmann⁴, Z. L. Hou¹, C. Hu²⁹, H. M. Hu¹, T. Hu^{1,a}, Y. Hu¹, G. S. Huang^{47,a}, J. S. Huang¹⁵, X. T. Huang³⁴, X. Z. Huang³⁰, Z. L. Huang²⁸, T. Hussain⁴⁹, W. Ikegami Andersson⁵¹, Q. Ji¹, Q. P. Ji¹⁵, X. B. Ji¹, X. L. Ji^{1,a}, X. S. Jiang^{1,a}, X. Y. Jiang³¹, J. B. Jiao³⁴, Z. Jiao¹⁷, D. P. Jin^{1,a}, S. Jin¹, T. Johansson⁵¹, A. Julin⁴⁵, N. Kalantar-Nayestanaki²⁶, X. L. Kang¹, X. S. Kang³¹, M. Kavatsyuk²⁶, B. C. Ke⁵, T. Khan^{47,a}, P. Kiese²³, R. Kliemt¹⁰, L. Koch²⁵, O. B. Kolcu^{42B,h}, B. Kopf⁴, M. Kornicer⁴⁴, M. Kuemmel⁴, M. Kuhlmann⁴, A. Kupsc⁵¹, W. Kühn²⁵, J. S. Lange²⁵, M. Lara¹⁹, P. Larin¹⁴, L. Lavezzi^{50C,1}, H. Leithoff²³, C. Leng^{50C}, C. Li⁵¹, Cheng Li^{47,a}, D. M. Li⁵⁴, F. Li^{1,a}, F. Y. Li³², G. Li¹, H. B. Li¹, H. J. Li¹, J. C. Li¹, Jin Li³³, K. Li¹³, K. Li³⁴, Lei Li³, P. L. Li^{47,a}, P. R. Li^{7,43}, Q. Y. Li³⁴, T. Li³⁴, W. D. Li¹, W. G. Li¹, X. L. Li³⁴, X. N. Li^{1,a}, X. Q. Li³¹, Z. B. Li⁴⁰, H. Liang^{47,a}, Y. F. Liang³⁷, Y. T. Liang²⁵, G. R. Liao¹¹, D. X. Lin¹⁴, B. Liu^{35,j}, B. J. Liu¹, C. X. Liu¹, D. Liu^{47,a}, F. H. Liu³⁶, Fang Liu¹, Feng Liu⁶, H. B. Liu¹², H. H. Liu¹⁶, H. H. Liu¹, H. M. Liu¹, J. B. Liu^{47,a}, J. P. Liu⁵², J. Y. Liu¹, K. Liu⁴¹, K. Y. Liu²⁸, Ke Liu⁶, L. D. Liu³², P. L. Liu^{1,a}, Q. Liu⁴³, S. B. Liu^{47,a}, X. Liu²⁷, Y. B. Liu³¹, Y. Y. Liu³¹, Z. A. Liu^{1,a}, Zhiqing Liu²³, Y. F. Long³², X. C. Lou^{1,a,g}, H. J. Lu¹⁷, J. G. Lu^{1,a}, Y. Lu¹, Y. P. Lu^{1,a}, C. L. Luo²⁹, M. X. Luo⁵³, T. Luo⁴⁴, X. L. Luo^{1,a}, X. R. Lyu⁴³, F. C. Ma²⁸, H. L. Ma¹, L. L. Ma³⁴, M. M. Ma¹, Q. M. Ma¹, T. Ma¹, X. N. Ma³¹, X. Y. Ma^{1,a}, Y. M. Ma³⁴, F. E. Maas¹⁴, M. Maggiora^{50A,50C}, Q. A. Malik⁴⁹, Y. J. Mao³², Z. P. Mao¹, S. Marcello^{50A,50C}, J. G. Messchendorp²⁶, G. Mezzadri^{21B}, J. Min^{1,a}, T. J. Min¹, R. E. Mitchell¹⁹, X. H. Mo^{1,a}, Y. J. Mo⁶, C. Morales Morales¹⁴, G. Morello^{20A}, N. Yu. Muchnoi^{9,e}, H. Muramatsu⁴⁵, P. Musiol⁴, A. Mustafa⁴, Y. Nefedov²⁴, F. Nerling¹⁰, I. B. Nikolaev^{9,e}, Z. Ning^{1,a}, S. Nisar⁸, S. L. Niu^{1,a}, X. Y. Niu¹, S. L. Olsen³³, Q. Ouyang^{1,a}, S. Pacetti^{20B}, Y. Pan^{47,a}, P. Patteri^{20A}, M. Pelizaeus⁴, J. Pellegrino^{50A,50C}, H. P. Peng^{47,a}, K. Peters^{10,i}, J. Pettersson⁵¹, J. L. Ping²⁹, R. G. Ping¹, R. Poling⁴⁵, V. Prasad^{39,47}, H. R. Qi², M. Qi³⁰, S. Qian^{1,a}, C. F. Qiao⁴³, J. J. Qin⁴³, N. Qin⁵², X. S. Qin¹, Z. H. Qin^{1,a}, J. F. Qiu¹, K. H. Rashid⁴⁹, C. F. Redmer²³, M. Richter⁴, M. Ripka²³, G. Rong¹, Ch. Rosner¹⁴, X. D. Ruan¹², A. Sarantsev^{24,f}, M. Savrić^{21B}, C. Schnier⁴, K. Schoenning⁵¹, W. Shan³², M. Shao^{47,a}, C. P. Shen², P. X. Shen³¹, X. Y. Shen¹, H. Y. Sheng¹, J. J. Song³⁴, X. Y. Song¹, S. Sosio^{50A,50C}, C. Sowa⁴, S. Spataro^{50A,50C}, G. X. Sun¹, J. F. Sun¹⁵, S. S. Sun¹, X. H. Sun¹, Y. J. Sun^{47,a}, Y. K. Sun^{47,a}, Y. Z. Sun¹, Z. J. Sun^{1,a}, Z. T. Sun¹⁹, C. J. Tang³⁷, G. Y. Tang¹, X. Tang¹, I. Tapan^{42C}, M. Tiemens²⁶, B. T. Tsednee²², I. Uman^{42D}, G. S. Varner⁴⁴, B. Wang¹, B. L. Wang⁴³, D. Wang³², D. Y. Wang³², Dan Wang⁴³, K. Wang^{1,a}, L. L. Wang¹, L. S. Wang¹, M. Wang³⁴, P. Wang¹, P. L. Wang¹, W. P. Wang^{47,a}, X. F. Wang⁴¹, Y. D. Wang¹⁴, Y. F. Wang^{1,a}, Y. Q. Wang²³, Z. Wang^{1,a}, Z. G. Wang^{1,a}, Z. H. Wang^{47,a}, Z. Y. Wang¹, Z. Y. Wang¹, T. Weber²³, D. H. Wei¹¹, P. Weidenkaff²³, S. P. Wen¹, U. Wiedner⁴, M. Wolke⁵¹, L. H. Wu¹, L. J. Wu¹, Z. Wu^{1,a}, L. Xia^{47,a}, Y. Xia¹⁸, D. Xiao¹, H. Xiao⁴⁸, Y. J. Xiao¹, Z. J. Xiao²⁹, Y. G. Xie^{1,a}, Y. H. Xie⁶, X. A. Xiong¹, Q. L. Xiu^{1,a}, G. F. Xu¹, J. J. Xu¹, L. Xu¹, Q. J. Xu¹³, Q. N. Xu⁴³, X. P. Xu³⁸, L. Yan^{50A,50C}, W. B. Yan^{47,a}, W. C. Yan^{47,a}, Y. H. Yan¹⁸, H. J. Yang^{35,j}, H. X. Yang¹, L. Yang⁵², Y. H. Yang³⁰, Y. X. Yang¹¹, M. Ye^{1,a}, M. H. Ye⁷, J. H. Yin¹, Z. Y. You⁴⁰, B. X. Yu^{1,a}, C. X. Yu³¹, J. S. Yu²⁷, C. Z. Yuan¹, Y. Yuan¹, A. Yuncu^{42B,b}, A. A. Zafar⁴⁹, Y. Zeng¹⁸, Z. Zeng^{47,a}, B. X. Zhang¹, B. Y. Zhang^{1,a}, C. C. Zhang¹, D. H. Zhang¹, H. H. Zhang⁴⁰, H. Y. Zhang^{1,a}, J. Zhang¹, J. L. Zhang¹, J. Q. Zhang¹, J. W. Zhang^{1,a}, J. Y. Zhang¹, J. Z. Zhang¹, K. Zhang¹, L. Zhang⁴¹, S. Q. Zhang³¹, X. Y. Zhang³⁴, Y. Zhang¹, Y. Zhang¹, Y. H. Zhang^{1,a}, Y. T. Zhang^{47,a}, Yu Zhang⁴³, Z. H. Zhang⁶, Z. P. Zhang⁴⁷, Z. Y. Zhang⁵², G. Zhao¹, J. W. Zhao^{1,a}, J. Y. Zhao¹, J. Z. Zhao^{1,a}, Lei Zhao^{47,a}, Ling Zhao¹, M. G. Zhao³¹, Q. Zhao¹, S. J. Zhao⁵⁴, T. C. Zhao¹, Y. B. Zhao^{1,a}, Z. G. Zhao^{47,a}, A. Zhemchugov^{24,c}, B. Zheng⁴⁸, J. P. Zheng^{1,a}, W. J. Zheng³⁴, Y. H. Zheng⁴³, B. Zhong²⁹, L. Zhou^{1,a}, X. Zhou⁵², X. K. Zhou^{47,a}, X. R. Zhou^{47,a}, X. Y. Zhou¹, Y. X. Zhou^{12,a}, K. Zhu¹, K. J. Zhu^{1,a}, S. Zhu¹, S. H. Zhu⁴⁶, X. L. Zhu⁴¹, Y. C. Zhu^{47,a}, Y. S. Zhu¹, Z. A. Zhu¹, J. Zhuang^{1,a}, L. Zotti^{50A,50C}, B. S. Zou¹, J. H. Zou¹

(BESIII Collaboration)

¹ Institute of High Energy Physics, Beijing 100049, People's Republic of China

² Beihang University, Beijing 100191, People's Republic of China

³ Beijing Institute of Petrochemical Technology, Beijing 102617, People's Republic of China

- ⁴ Bochum Ruhr-University, D-44780 Bochum, Germany
- ⁵ Carnegie Mellon University, Pittsburgh, Pennsylvania 15213, USA
- ⁶ Central China Normal University, Wuhan 430079, People's Republic of China
- ⁷ China Center of Advanced Science and Technology, Beijing 100190, People's Republic of China
- ⁸ COMSATS Institute of Information Technology, Lahore, Defence Road, Off Raiwind Road, 54000 Lahore, Pakistan
- ⁹ G.I. Budker Institute of Nuclear Physics SB RAS (BINP), Novosibirsk 630090, Russia
- ¹⁰ GSI Helmholtzcentre for Heavy Ion Research GmbH, D-64291 Darmstadt, Germany
- ¹¹ Guangxi Normal University, Guilin 541004, People's Republic of China
- ¹² Guangxi University, Nanning 530004, People's Republic of China
- ¹³ Hangzhou Normal University, Hangzhou 310036, People's Republic of China
- ¹⁴ Helmholtz Institute Mainz, Johann-Joachim-Becher-Weg 45, D-55099 Mainz, Germany
- ¹⁵ Henan Normal University, Xinxiang 453007, People's Republic of China
- ¹⁶ Henan University of Science and Technology, Luoyang 471003, People's Republic of China
- ¹⁷ Huangshan College, Huangshan 245000, People's Republic of China
- ¹⁸ Hunan University, Changsha 410082, People's Republic of China
- ¹⁹ Indiana University, Bloomington, Indiana 47405, USA
- ²⁰ (A)INFN Laboratori Nazionali di Frascati, I-00044, Frascati, Italy; (B)INFN and University of Perugia, I-06100, Perugia, Italy
- ²¹ (A)INFN Sezione di Ferrara, I-44122, Ferrara, Italy; (B)University of Ferrara, I-44122, Ferrara, Italy
- ²² Institute of Physics and Technology, Peace Ave. 54B, Ulaanbaatar 13330, Mongolia
- ²³ Johannes Gutenberg University of Mainz, Johann-Joachim-Becher-Weg 45, D-55099 Mainz, Germany
- ²⁴ Joint Institute for Nuclear Research, 141980 Dubna, Moscow region, Russia
- ²⁵ Justus-Liebig-Universitaet Giessen, II. Physikalisches Institut, Heinrich-Buff-Ring 16, D-35392 Giessen, Germany
- ²⁶ KVI-CART, University of Groningen, NL-9747 AA Groningen, The Netherlands
- ²⁷ Lanzhou University, Lanzhou 730000, People's Republic of China
- ²⁸ Liaoning University, Shenyang 110036, People's Republic of China
- ²⁹ Nanjing Normal University, Nanjing 210023, People's Republic of China
- ³⁰ Nanjing University, Nanjing 210093, People's Republic of China
- ³¹ Nankai University, Tianjin 300071, People's Republic of China
- ³² Peking University, Beijing 100871, People's Republic of China
- ³³ Seoul National University, Seoul, 151-747 Korea
- ³⁴ Shandong University, Jinan 250100, People's Republic of China
- ³⁵ Shanghai Jiao Tong University, Shanghai 200240, People's Republic of China
- ³⁶ Shanxi University, Taiyuan 030006, People's Republic of China
- ³⁷ Sichuan University, Chengdu 610064, People's Republic of China
- ³⁸ Soochow University, Suzhou 215006, People's Republic of China
- ³⁹ State Key Laboratory of Particle Detection and Electronics, Beijing 100049, Hefei 230026, People's Republic of China
- ⁴⁰ Sun Yat-Sen University, Guangzhou 510275, People's Republic of China
- ⁴¹ Tsinghua University, Beijing 100084, People's Republic of China
- ⁴² (A)Ankara University, 06100 Tandogan, Ankara, Turkey; (B)Istanbul Bilgi University, 34060 Eyup, Istanbul, Turkey; (C)Uludag University, 16059 Bursa, Turkey; (D)Near East University, Nicosia, North Cyprus, Mersin 10, Turkey
- ⁴³ University of Chinese Academy of Sciences, Beijing 100049, People's Republic of China
- ⁴⁴ University of Hawaii, Honolulu, Hawaii 96822, USA
- ⁴⁵ University of Minnesota, Minneapolis, Minnesota 55455, USA
- ⁴⁶ University of Science and Technology Liaoning, Anshan 114051, People's Republic of China
- ⁴⁷ University of Science and Technology of China, Hefei 230026, People's Republic of China
- ⁴⁸ University of South China, Hengyang 421001, People's Republic of China
- ⁴⁹ University of the Punjab, Lahore-54590, Pakistan
- ⁵⁰ (A)University of Turin, I-10125, Turin, Italy; (B)University of Eastern Piedmont, I-15121, Alessandria, Italy; (C)INFN, I-10125, Turin, Italy
- ⁵¹ Uppsala University, Box 516, SE-75120 Uppsala, Sweden
- ⁵² Wuhan University, Wuhan 430072, People's Republic of China
- ⁵³ Zhejiang University, Hangzhou 310027, People's Republic of China
- ⁵⁴ Zhengzhou University, Zhengzhou 450001, People's Republic of China

^a Also at State Key Laboratory of Particle Detection and Electronics, Beijing 100049, Hefei 230026, People's Republic of China

^b Also at Bogazici University, 34342 Istanbul, Turkey

^c Also at the Moscow Institute of Physics and Technology, Moscow 141700, Russia

^d Also at the Functional Electronics Laboratory, Tomsk State University, Tomsk, 634050, Russia

^e Also at the Novosibirsk State University, Novosibirsk, 630090, Russia

^f Also at the NRC “Kurchatov Institute”, PNPI, 188300, Gatchina, Russia

^g Also at University of Texas at Dallas, Richardson, Texas 75083, USA

^h Also at Istanbul Arel University, 34295 Istanbul, Turkey

ⁱ Also at Goethe University Frankfurt, 60323 Frankfurt am Main, Germany

^j Also at Key Laboratory for Particle Physics, Astrophysics and Cosmology, Ministry of Education; Shanghai Key Laboratory for Particle Physics and Cosmology; Institute of Nuclear and Particle Physics, Shanghai 200240, People’s Republic of China

Abstract

We report the first observation of the decay $\Lambda_c^+ \rightarrow \Sigma^- \pi^+ \pi^+ \pi^0$, based on data obtained in e^+e^- annihilations with an integrated luminosity of 567 pb^{-1} at $\sqrt{s} = 4.6 \text{ GeV}$. The data were collected with the BESIII detector at the BEPCII storage rings. The absolute branching fraction $\mathcal{B}(\Lambda_c^+ \rightarrow \Sigma^- \pi^+ \pi^+ \pi^0)$ is determined to be $(2.11 \pm 0.33(\text{stat.}) \pm 0.14(\text{syst.}))\%$. In addition, an improved measurement of $\mathcal{B}(\Lambda_c^+ \rightarrow \Sigma^- \pi^+ \pi^+)$ is determined as $(1.81 \pm 0.17(\text{stat.}) \pm 0.09(\text{syst.}))\%$.

Keywords: branching fraction, charmed baryon, weak decays, e^+e^- annihilation, BESIII

1. Introduction

The study of hadronic decays of charmed baryons provides important information to understand both the strong and the weak interactions [1]. It also provides essential input to understand background contributions in the study of b -baryon physics, as Λ_b decays dominantly to Λ_c^+ . More than 30 years have passed since the Λ_c^+ baryon was first observed in e^+e^- annihilations by the Mark II experiment [2] and the knowledge of Λ_c^+ decays remains very poor compared to that for charmed mesons. So far, measured decay modes account for only about 60% [3] of all Λ_c^+ decays, primarily consisting of modes with a $\Lambda(\Sigma)$ hyperon or a proton in the final state. Decays to the Σ^- hyperon are Cabibbo-allowed and are expected to have large rates. However, no experimental measurements exist except for $\Lambda_c^+ \rightarrow \Sigma^- \pi^+ \pi^+$ [3]. Therefore, searching for additional decay modes with Σ^- in the final state is important to build up knowledge on Λ_c^+ decays. In this paper, we report the first observation of the so-far undetermined, but expected to be large, decay of $\Lambda_c^+ \rightarrow \Sigma^- \pi^+ \pi^+ \pi^0$ [4]. In addition, we perform the first absolute measurement of the branching fraction for $\Lambda_c^+ \rightarrow \Sigma^- \pi^+ \pi^+$.

The data analyzed in this work corresponds to an integrated luminosity of 567 pb^{-1} [5] of e^+e^- annihilations at center-of-mass energy (c.m.) $\sqrt{s} = 4.6 \text{ GeV}$

by the BEPCII collider and collected with the BESIII detector [6]. The c.m. energy is slightly above the threshold for the production of $\Lambda_c^+ \bar{\Lambda}_c^-$, so $\Lambda_c^+ \bar{\Lambda}_c^-$ pairs are produced with no additional hadrons. The analysis technique in this work, which was first applied in the Mark III experiment [7], is optimized for measuring charm hadron pairs produced near threshold. First, we select the subset of our events in which a $\bar{\Lambda}_c^-$ is reconstructed in an exclusive hadronic decay mode, designated as the single-tag (ST) sample. Events in this ST sample are then searched for the signal channel $\Lambda_c^+ \rightarrow \Sigma^- \pi^+ \pi^+ (\pi^0)$ in the system recoiling against the ST to select double tag (DT) events. In the final states of $\Lambda_c^+ \rightarrow \Sigma^- \pi^+ \pi^+ (\pi^0)$, the Σ^- hyperon is detected through $\Sigma^- \rightarrow n \pi^-$. As the neutron is not reconstructed in this analysis, we deduce its kinematic properties by four-momentum conservation. The absolute branching fraction (BF) of $\Lambda_c^+ \rightarrow \Sigma^- \pi^+ \pi^+ (\pi^0)$ is derived from the probability of detecting the DT signals in the ST sample. Hence, this method provides a clean and straightforward BF measurement that is independent of the number of $\Lambda_c^+ \bar{\Lambda}_c^-$ events produced.

2. BESIII Detector and Monte Carlo Simulation

BESIII [6] is a cylindrical detector with a coverage of 93% of the full 4π solid angle. It consists of a

Helium-gas based main drift chamber (MDC), a plastic scintillator time-of-flight (TOF) system, a CsI (TI) electromagnetic calorimeter (EMC), a superconducting solenoid providing a 1.0 T magnetic field, and a muon detection system in the iron flux return of the magnet. The charged particle momentum resolution is 0.5% at a transverse momentum of 1 GeV/c. The photon energy resolution at 1 GeV is 2.5% in the central barrel region and 5.0% in the two end caps. More details about the design and performance of the detector are given in Ref. [6].

A GEANT4-based [8] Monte Carlo (MC) simulation package, which includes the geometric description of the detector and the detector response, is used to determine the detection efficiency and to estimate the potential backgrounds. MC samples of the signal mode $\Lambda_c^+ \rightarrow \Sigma^- \pi^+ \pi^+ (\pi^0)$, together with a $\bar{\Lambda}_c^-$ decaying to specified ST modes, are generated with KKMC [9] and EVTGEN [10], taking into account initial-state radiation (ISR) [11] and final-state radiation [12] effects. The $\Lambda_c^+ \rightarrow \Sigma^- \pi^+ \pi^+ (\pi^0)$ decay is simulated by reweighting the phase-space-generated MC events to approximate observed kinematic distributions in data. To understand potential background contributions, an inclusive MC sample is used. It includes generic $\Lambda_c^+ \bar{\Lambda}_c^-$ events, $D_{(s)}^{(*)} \bar{D}_{(s)}^{(*)} + X$ production, ISR return to the charmonium states at lower masses and continuum $q\bar{q}$ processes. Previously measured decay modes of the Λ_c , ψ and $D_{(s)}$ are simulated with EVTGEN, using BFs from the Particle Data Group (PDG) [3]. The unknown decays of the ψ states are generated with LUND-CHARM [13].

3. Analysis

The ST and DT selection technique that is used in our analysis follows closely the one used and described in Ref. [14]. We reconstruct the $\bar{\Lambda}_c^-$ baryons in the eleven hadronic decay modes listed in Table 1. Intermediate particles are reconstructed through their decays $K_S^0 \rightarrow \pi^+ \pi^-$, $\bar{\Lambda} \rightarrow \bar{p} \pi^+$, $\bar{\Sigma}^0 \rightarrow \gamma \bar{\Lambda}$ with $\bar{\Lambda} \rightarrow \bar{p} \pi^+$, $\bar{\Sigma}^- \rightarrow \bar{p} \pi^0$, and $\pi^0 \rightarrow \gamma \gamma$. The selection criteria for the proton, kaon, pion, π^0 , K_S^0 and $\bar{\Lambda}$ candidates used in the reconstruction of the ST signals are described in Ref. [14].

The ST $\bar{\Lambda}_c^-$ signals are identified using the beam-energy-constrained mass, $M_{BC} = \sqrt{E_{\text{beam}}^2 - |\vec{p}_{\bar{\Lambda}_c^-}|^2}$, where E_{beam} is the beam energy and $\vec{p}_{\bar{\Lambda}_c^-}$ is the momentum of the $\bar{\Lambda}_c^-$ candidate in the rest frame of the initial e^+e^- system [15]. To improve the signal purity, the energy difference $\Delta E = E_{\text{beam}} - E_{\bar{\Lambda}_c^-}$ for

each candidate is required to be within approximately $\pm 3\sigma$ of the ΔE signal peak position, where σ is the ΔE resolution and $E_{\bar{\Lambda}_c^-}$ is the reconstructed $\bar{\Lambda}_c^-$ energy. Table 1 shows the mode-dependent ΔE requirements and the ST yields in the M_{BC} signal region (2.280, 2.296) GeV/ c^2 , which are obtained by fits to the M_{BC} distributions. See Ref. [14] for more details. The total ST yield is $N_{\bar{\Lambda}_c^-}^{\text{tot}} = 14415 \pm 159$, where the uncertainty is statistical only.

Candidates for the decay $\Lambda_c^+ \rightarrow \Sigma^- \pi^+ \pi^+ (\pi^0)$ with $\Sigma^- \rightarrow n \pi^-$ are reconstructed from the tracks not used in the ST $\bar{\Lambda}_c^-$ reconstruction. It is required that there are only three charged tracks in the system recoiling against the $\bar{\Lambda}_c^-$ satisfying $|\cos \theta| < 0.93$, where θ is the polar angle with respect to the beam direction. For the two π^+ candidates from the Λ_c^+ , the distances of closest approach to the interaction point must be within ± 10 cm along the beam direction and within 1 cm in the perpendicular plane, while the π^- candidate from Σ^- decay is not subjected to this requirement. Identification of charged tracks is performed by combining the dE/dx information from the MDC and the time of flight measured in the TOF to obtain the probability \mathcal{L}_h for each hadron type h . The three charged pions must satisfy $\mathcal{L}_\pi > \mathcal{L}_K$. Photon candidates are reconstructed from isolated clusters in the EMC in the regions $|\cos \theta| \leq 0.80$ (barrel) and $0.86 \leq |\cos \theta| \leq 0.92$ (end cap). The deposited energy of a neutral cluster is required to be larger than 25 (50) MeV in the barrel (end cap) region, and the angle between the photon candidate and the nearest charged track must be larger than 10° . To suppress electronic noise and energy deposits unrelated to the event, the difference between the EMC time and the event start time is required to be within (0, 700) ns. To reconstruct π^0 candidates, the invariant mass of photon pairs is required to be within (0.110, 0.155) GeV/ c^2 and, as a second step, a kinematic fit is implemented to constrain the $\gamma\gamma$ invariant mass to the nominal π^0 mass [3].

The kinematic variable

$$M_n = \sqrt{(E_{\text{beam}} - E_{\pi^+ \pi^+ \pi^- (\pi^0)})^2 - |\vec{p}_{\Lambda_c^+} - \vec{p}_{\pi^+ \pi^+ \pi^- (\pi^0)}|^2}$$

is computed to characterize the reconstructed mass of the undetected neutron, where $E_{\pi^+ \pi^+ \pi^- (\pi^0)}$ is the energy of the $\pi^+ \pi^+ \pi^- (\pi^0)$ combination and $\vec{p}_{\pi^+ \pi^+ \pi^- (\pi^0)}$ is the three-momentum of the $\pi^+ \pi^+ \pi^- (\pi^0)$ combination. The expected momentum $\vec{p}_{\Lambda_c^+}$ of the Λ_c^+ is calculated by $\vec{p}_{\Lambda_c^+} = -\hat{p}_{\text{tag}} \sqrt{E_{\text{beam}}^2 - m_{\Lambda_c^+}^2}$, where \hat{p}_{tag} is the direction of the momentum of the ST $\bar{\Lambda}_c^-$ candidate and $m_{\Lambda_c^+}$ is the mass of the Λ_c^+ taken from the PDG [3]. Similarly, we

Table 1: Requirements on ΔE and ST yields $N_{\Lambda_c^-}$ for the eleven ST modes. The uncertainties are statistical only.

Mode	ΔE (GeV)	$N_{\Lambda_c^-}$
$\bar{p}K_S^0$	$[-0.025, 0.028]$	1066 ± 33
$\bar{p}K^+\pi^-$	$[-0.019, 0.023]$	5692 ± 88
$\bar{p}K_S^0\pi^0$	$[-0.035, 0.049]$	593 ± 41
$\bar{p}K^+\pi^-\pi^0$	$[-0.044, 0.052]$	1547 ± 61
$\bar{p}K_S^0\pi^+\pi^-$	$[-0.029, 0.032]$	516 ± 34
$\bar{\Lambda}\pi^-$	$[-0.033, 0.035]$	593 ± 25
$\bar{\Lambda}\pi^-\pi^0$	$[-0.037, 0.052]$	1864 ± 56
$\bar{\Lambda}\pi^-\pi^+\pi^-$	$[-0.028, 0.030]$	674 ± 36
$\bar{\Sigma}^0\pi^-$	$[-0.029, 0.032]$	532 ± 30
$\bar{\Sigma}^-\pi^0$	$[-0.038, 0.062]$	329 ± 28
$\bar{\Sigma}^-\pi^+\pi^-$	$[-0.049, 0.054]$	1009 ± 57

can construct the variable

$$M_{n\pi^-} = \sqrt{(E_{\text{beam}} - E_{\pi^+\pi^+(\pi^0)})^2 - |\vec{p}_{\Lambda_c^+} - \vec{p}_{\pi^+\pi^+(\pi^0)}|^2}$$

to represent the reconstructed mass of the Σ^- .

The distributions of M_n versus $M_{n\pi^-}$ for the $\Lambda_c^+ \rightarrow \Sigma^-\pi^+\pi^+$ and $\Lambda_c^+ \rightarrow \Sigma^-\pi^+\pi^+\pi^0$ candidates in data are shown in Figs. 1 (a) and (b), respectively, where clusters corresponding to signal decays are evident. To improve the resolution of the signal mass, as well as to better handle the backgrounds around the Σ^- and neutron mass regions, we determine the signal yields from the distribution of the mass difference $M_{n\pi^-} - M_n$, since $M_{n\pi^-}$ and M_n are highly correlated. Based on a study of the inclusive MC samples, no peaking backgrounds are expected for these two channels. We perform an unbinned maximum likelihood fit to the $M_{n\pi^-} - M_n$ spectra, as shown in Figs. 1 (c) and (d). In the fits, the signals are described by non-parametric functions extracted from the signal MC convoluted with a Gaussian function accounting for the resolution difference between data and MC, while the background shapes are described with a second-order polynomial function. The width of the Gaussian is left free in the fit, while its mean is fixed to zero. From the fits, we find the DT signal yields $N_{\Sigma^-\pi^+\pi^+}^{\text{obs}} = 161 \pm 15$ and $N_{\Sigma^-\pi^+\pi^+\pi^0}^{\text{obs}} = 88 \pm 14$, where the uncertainties are statistical only. Backgrounds from non- Λ_c^+ decays are estimated by examining the ST candidates in the M_{BC} side-band (2.252, 2.272) GeV/ c^2 in data. The backgrounds from non- Λ_c^+ decays are found to be negligible.

The absolute BF's for $\Lambda_c^+ \rightarrow \Sigma^-\pi^+\pi^+$ and $\Lambda_c^+ \rightarrow$

$\Sigma^-\pi^+\pi^+\pi^0$ are determined by

$$\mathcal{B}(\Lambda_c^+ \rightarrow \Sigma^-\pi^+\pi^+(\pi^0)) = \frac{N_{\Sigma^-\pi^+\pi^+(\pi^0)}^{\text{obs}}}{N_{\Lambda_c^+}^{\text{tot}} \cdot \varepsilon_{\Sigma^-\pi^+\pi^+(\pi^0)} \cdot \mathcal{B}(\Sigma^- \rightarrow n\pi^-)}, \quad (1)$$

where $\varepsilon_{\Sigma^-\pi^+\pi^+(\pi^0)}$ is the detection efficiency for the $\Lambda_c^+ \rightarrow \Sigma^-\pi^+\pi^+(\pi^0)$ decay with $\Sigma^- \rightarrow n\pi^-$. The intermediate decay branching fraction of $\Sigma^- \rightarrow n\pi^-$ is included in the denominator of Eq. (1). For each ST mode i , the efficiency $\varepsilon_{\Sigma^-\pi^+\pi^+(\pi^0)}^i$ is obtained by dividing the DT efficiency $\varepsilon_{\text{tag}, \Sigma^-\pi^+\pi^+(\pi^0)}^i$ by the ST efficiency $\varepsilon_{\text{tag}}^i$. After weighting $\varepsilon_{\Sigma^-\pi^+\pi^+(\pi^0)}^i$ by the mode-by-mode ST yields in data, we find the overall average efficiencies $\varepsilon_{\Sigma^-\pi^+\pi^+} = (61.8 \pm 0.4)\%$ and $\varepsilon_{\Sigma^-\pi^+\pi^+\pi^0} = (29.0 \pm 0.2)\%$, where the branching fraction for $\pi^0 \rightarrow \gamma\gamma$ is included. Substituting the values of $N_{\Sigma^-\pi^+\pi^+(\pi^0)}^{\text{obs}}$, $N_{\Lambda_c^+}^{\text{tot}}$, $\varepsilon_{\Sigma^-\pi^+\pi^+(\pi^0)}$ and $\mathcal{B}(\Sigma^- \rightarrow n\pi^-)$ in Eq. (1), we obtain $\mathcal{B}(\Lambda_c^+ \rightarrow \Sigma^-\pi^+\pi^+) = (1.81 \pm 0.17 \pm 0.09)\%$ and $\mathcal{B}(\Lambda_c^+ \rightarrow \Sigma^-\pi^+\pi^+\pi^0) = (2.11 \pm 0.33 \pm 0.14)\%$, where the first uncertainties are statistical, and the second are systematic, as described below.

With the DT technique, the BF measurement is insensitive to uncertainty in the ST efficiencies. The systematic uncertainties in measuring $\mathcal{B}(\Lambda_c^+ \rightarrow \Sigma^-\pi^+\pi^+)$ and $\mathcal{B}(\Lambda_c^+ \rightarrow \Sigma^-\pi^+\pi^+\pi^0)$ mainly arise from the efficiencies of π detection and identification, fits to the $M_{n\pi^-} - M_n$ distributions and the signal modelling in the MC simulation. The systematic uncertainties in the π^\pm tracking and identification are both determined to be 1.0% by studying a set of samples of $e^+e^- \rightarrow \pi^+\pi^-\pi^+\pi^-$, $e^+e^- \rightarrow K^+K^-\pi^+\pi^-$ and $e^+e^- \rightarrow p\bar{p}\pi^+\pi^-$ obtained from data with c.m. en-

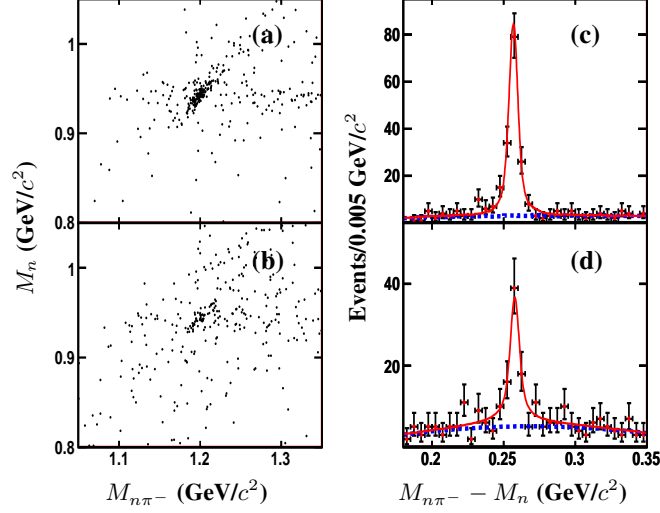


Fig. 1: Scatter plots of M_n versus $M_{n\pi^-}$ for candidates in data for (a) $\Lambda_c^+ \rightarrow \Sigma^- \pi^+ \pi^+$ and (b) $\Lambda_c^+ \rightarrow \Sigma^- \pi^+ \pi^+ \pi^0$. Also shown are fits to the distributions of $M_{n\pi^-} - M_n$ for (c) $\Lambda_c^+ \rightarrow \Sigma^- \pi^+ \pi^+$ and (d) $\Lambda_c^+ \rightarrow \Sigma^- \pi^+ \pi^+ \pi^0$ in data. Solid lines are the results of a complete fit while dashed lines reflect the background components.

ergy above 4.0 GeV. The π^0 reconstruction efficiency is validated by analyzing DT events with $\bar{D}^0 \rightarrow K^+ \pi^-$ or $K^+ \pi^- \pi^0$ versus $D^0 \rightarrow K^- \pi^+ \pi^0$ [16]. The difference of the π^0 reconstruction efficiencies between data and MC simulations is estimated to be 2.0%. The uncertainty from the fit to the $M_{n\pi^-} - M_n$ distribution is evaluated by checking the relative changes of $N_{\Sigma^- \pi^+ \pi^+ (\pi^0)}^{\text{obs}}$ with different choices for signal shapes (double Gaussian function), background shapes (first-order polynomial function, third-order polynomial function and a MC-derived background shape) and fit ranges ((0.19, 0.34) GeV/ c^2). The uncertainty in modelling the signal process is obtained by varying the reweighting factors of the observed kinematic variables within their statistical uncertainties and extracting the difference of the resultant efficiencies. The difference is estimated to be 2.0% for the studied channels and is taken as the systematic uncertainty due to the signal modelling. In addition, there are systematic uncertainties in obtaining $N_{\Lambda_c^+}^{\text{tot}}$ evaluated by using alternative signal shapes in the fits to the M_{BC} spectra [14], resulting in an uncertainty of 1.0%, and in the statistical limitation of the MC samples, which is estimated to be 0.6 (0.7)% for $\Lambda_c^+ \rightarrow \Sigma^- \pi^+ \pi^+ (\pi^0)$. The uncertainties from the BF of $\Sigma^- \rightarrow n \pi^-$ and $\pi^0 \rightarrow \gamma \gamma$ are negligible. All of the above systematic uncertainties are summarized in Table 2, and the total uncertainties are evaluated to be 5.2% and 6.4% for $\mathcal{B}(\Lambda_c^+ \rightarrow \Sigma^- \pi^+ \pi^+)$ and $\mathcal{B}(\Lambda_c^+ \rightarrow \Sigma^- \pi^+ \pi^+ \pi^0)$, respectively, by combining all

items in quadrature.

4. Summary

Based on an e^+e^- collision data sample with an integrated luminosity of 567 pb $^{-1}$ taken at $\sqrt{s} = 4.6$ GeV with the BESIII detector, we report the first observation of the decay $\Lambda_c^+ \rightarrow \Sigma^- \pi^+ \pi^+ \pi^0$ and the first absolute BF measurement for $\Lambda_c^+ \rightarrow \Sigma^- \pi^+ \pi^+$. The results are $\mathcal{B}(\Lambda_c^+ \rightarrow \Sigma^- \pi^+ \pi^+) = (1.81 \pm 0.17 \pm 0.09)\%$ and $\mathcal{B}(\Lambda_c^+ \rightarrow \Sigma^- \pi^+ \pi^+ \pi^0) = (2.11 \pm 0.33 \pm 0.14)\%$, where the first uncertainties are statistical and the second are systematic.

Our result for $\mathcal{B}(\Lambda_c^+ \rightarrow \Sigma^- \pi^+ \pi^+)$ is consistent with and more precise than the previous result [3]. BESIII measured the BF of the isospin symmetric channel $\mathcal{B}(\Lambda_c^+ \rightarrow \Sigma^+ \pi^+ \pi^-) = (4.25 \pm 0.24 \pm 0.20)\%$ [17]. This allows us to determine the ratio $\mathcal{B}(\Lambda_c^+ \rightarrow \Sigma^- \pi^+ \pi^+)/\mathcal{B}(\Lambda_c^+ \rightarrow \Sigma^+ \pi^+ \pi^-) = 0.42 \pm 0.05 \pm 0.02$, where the first uncertainty is statistical and the second systematic. The statistical uncertainty of the ratio dominates, as many common systematic uncertainties cancel. This is consistent with and more precise than the value previously measured by the E687 Collaboration ($0.53 \pm 0.15 \pm 0.07$) [18].

5. Acknowledgments

The BESIII collaboration thanks the staff of BEPCII and the IHEP computing center for their strong sup-

Table 2: Summary of the relative systematic uncertainties $\Delta_{\Sigma^-\pi^+\pi^+}^{\text{syst}}$ and $\Delta_{\Sigma^-\pi^+\pi^+\pi^0}^{\text{syst}}$ in $\mathcal{B}(\Lambda_c^+ \rightarrow \Sigma^-\pi^+\pi^+)$ and $\mathcal{B}(\Lambda_c^+ \rightarrow \Sigma^-\pi^+\pi^+\pi^0)$, respectively.

Source	$\Delta_{\Sigma^-\pi^+\pi^+}^{\text{syst}} [\%]$	$\Delta_{\Sigma^-\pi^+\pi^+\pi^0}^{\text{syst}} [\%]$
π^\pm tracking	3.0	3.0
π^\pm identification	3.0	3.0
π^0 reconstruction	...	2.0
Fit to $M_n - M_{n\pi^-}$	2.0	3.6
Signal modelling	2.0	2.0
MC statistics	0.6	0.7
$N_{\Lambda_c^-}^{\text{tot}}$	1.0	1.0
Total	5.2	6.4

port. This work is supported in part by National Key Basic Research Program of China under Contract No. 2015CB856700; National Natural Science Foundation of China (NSFC) under Contracts Nos. 11125525, 11235011, 11275266, 11305180, 11322544, 11322544, 11335008, 11425524, 11505010; the Chinese Academy of Sciences (CAS) Large-Scale Scientific Facility Program; the CAS Center for Excellence in Particle Physics (CCEPP); Joint Large-Scale Scientific Facility Funds of the NSFC and CAS under Contracts Nos. U1332201, U1532257, U1532258; CAS under Contracts Nos. KJCX2-YW-N29, KJCX2-YW-N45, QYZDJ-SSW-SLH003; 100 Talents Program of CAS; National 1000 Talents Program of China; INPAC and Shanghai Key Laboratory for Particle Physics and Cosmology; German Research Foundation DFG under Contracts Nos. Collaborative Research Center CRC 1044, FOR 2359; Istituto Nazionale di Fisica Nucleare, Italy; Joint Large-Scale Scientific Facility Funds of the NSFC and CAS; Koninklijke Nederlandse Akademie van Wetenschappen (KNAW) under Contract No. 530-4CDP03; Ministry of Development of Turkey under Contract No. DPT2006K-120470; National Science and Technology fund; The Swedish Resarch Council; U.S. Department of Energy under Contracts Nos. DE-FG02-05ER41374, DE-SC-0010118, DE-SC-0010504, DE-SC-0012069; University of Groningen (RuG) and the Helmholtzzentrum fuer Schwerionenforschung GmbH (GSI), Darmstadt; WCU Program of National Research Foundation of Korea under Contract No. R32-2008-000-10155-0. This paper is also supported by Beijing municipal government under Contract Nos. KM201610017009, 2015000020124G064.

References

- [1] H. Y. Cheng, Charmed baryons circa 2015, *Front. Phys.* **10**(6) (2015) 101406, <https://link.springer.com/>

- [article/10.1007/s11467-015-0483-z](https://doi.org/10.1007/s11467-015-0483-z); C. D. Lü, W. Wang and F. S. Yu, Test flavor SU(3) symmetry in exclusive Λ_c decays *Phys. Rev. D* **93** (2016) 056008, <https://doi.org/10.1103/PhysRevD.93.056008>, arXiv:1601.04241; K. K. Sharma and R. C. Verma, SU(3)_{flavor} analysis of two-body weak decays of charmed baryons, *Phys. Rev. D* **55** (1997) 7067, <https://doi.org/10.1103/PhysRevD.55.7067>, hep-ph/9704391; L. L. Chau, H. Y. Cheng and B. Tseng, Analysis of two-body decays of charmed baryons using the quark-diagram scheme, *Phys. Rev. D* **54** (1996) 2132, <https://doi.org/10.1103/PhysRevD.54.2132>, hep-ph/9508382.
- [2] G. S. Abrams *et al.*, Mark II Collaboration, Observation of Charmed-Baryon Production in e^+e^- Annihilation, *Phys. Rev. Lett.* **44** (1980) 10, <https://doi.org/10.1103/PhysRevLett.44.10>.
- [3] C. Patrignani *et al.*, Particle Data Group, Review of Particle Physics, *Chin. Phys. C* **40** (2016) 100001, <http://dx.doi.org/10.1088/1674-1137/40/10/100001>.
- [4] Throughout this paper, charged conjugate modes are implied unless explicitly stated otherwise.
- [5] M. Ablikim, *et al.*, BESIII Collaboration, Precision measurement of the integrated luminosity of the data taken by BESIII at center-of-mass energies between 3.810 GeV and 4.600 GeV, *Chin. Phys. C* **39** (2015) 093001, <http://iopscience.iop.org/1674-1137/39/9/093001>, arXiv:1503.03408.
- [6] M. Ablikim, *et al.*, BESIII Collaboration, Design and Construction of the BESIII Detector, *Nucl. Instrum. Meth. A* **614** (2010) 345, <http://dx.doi.org/10.1016/j.nima.2009.12.050>, arXiv:0911.4960.
- [7] J. Adler *et al.*, Mark III Collaboration, Measurement of the branching fractions for $D^0 \rightarrow \pi^- e^+ \nu_e$ and $D^0 \rightarrow K^- e^+ \nu_e$ and determination of $|V_{cd}/V_{cs}|^2$, *Phys. Rev. Lett.* **62** (1989) 1821, <http://dx.doi.org/10.1103/PhysRevLett.62.1821>.
- [8] S. Agostinelli, *et al.*, GEANT4 Collaboration, GEANT4-A Simulation toolkit, *Nucl. Instrum. Meth. A* **506** (2003) 250, [http://dx.doi.org/10.1016/S0168-9002\(03\)01368-8](http://dx.doi.org/10.1016/S0168-9002(03)01368-8).
- [9] S. Jadach, B. F. L. Ward and Z. Was, The precision Monte Carlo event generator *KK* for two-fermion final states in e^+e^- collisions, *Comput. Phys. Commun.* **130** (2000) 260, [http://dx.doi.org/10.1016/S0010-4655\(00\)00048-5](http://dx.doi.org/10.1016/S0010-4655(00)00048-5), arXiv:hep-ph/9912214; Coherent exclusive exponentiation for precision Monte Carlo calculations, *Phys. Rev. D* **63** (2001) 113009, <https://doi.org/10.1103/PhysRevD.63.113009>, arXiv:hep-

- ph/0006359.
- [10] D. J. Lange, The EvtGen particle decay simulation package, Nucl. Instrum. Meth. A **462** (2001) 152, [http://dx.doi.org/10.1016/S0168-9002\(01\)00089-4](http://dx.doi.org/10.1016/S0168-9002(01)00089-4).
 - [11] E. A. Kuraev and V. S. Fadin, Radiative corrections to the cross section for single-photon annihilation of an e^+e^- pair at high energy, Sov. J. Nucl. Phys. **41** (1985) 466, [http://refhub.elsevier.com/S0370-2693\(17\)30065-5/bib534A4E5034315F343636s1](http://refhub.elsevier.com/S0370-2693(17)30065-5/bib534A4E5034315F343636s1).
 - [12] E. Richter-Was, QED bremsstrahlung in semileptonic B and leptonic τ decays, Phys. Lett. B **303** (1993) 163, [http://dx.doi.org/10.1016/0370-2693\(93\)90062-M](http://dx.doi.org/10.1016/0370-2693(93)90062-M); E. Barberio and Z. Was, PHOTOS-a universal Monte Carlo for QED radiative corrections: version 2.0, Comput. Phys. Commun. **79** (1994) 291, [http://dx.doi.org/10.1016/0010-4655\(94\)90074-4](http://dx.doi.org/10.1016/0010-4655(94)90074-4).
 - [13] J. C. Chen, G. S. Huang, X. R. Qi, D. H. Zhang, Y. S. Zhu, Event generator for J/ψ and $\psi(2S)$ decay, Phys. Rev. D **62** (2000) 034003, <https://doi.org/10.1103/PhysRevD.62.034003>.
 - [14] M. Ablikim, et al., BESIII Collaboration, Measurement of the Absolute Branching Fraction for $\Lambda_c^+ \rightarrow \Lambda e^+ \nu_e$, Phys. Rev. Lett. **115** (2015) 221805, <https://doi.org/10.1103/PhysRevLett.115.221805>, arXiv:1510.02610; Measurement of the Absolute Branching Fraction for $\Lambda_c^+ \rightarrow \Lambda \mu^+ \nu_\mu$, Phys. Lett. B **767** (2017) 42, <http://dx.doi.org/10.1016/j.physletb.2017.01.047>, arXiv:1611.04382; Observation of $\Lambda_c^+ \rightarrow n K_S^0 \pi^+$, Phys. Rev. Lett. **118** (2017) 112001, <http://dx.doi.org/10.1103/PhysRevLett.118.112001>, arXiv:1611.02797.
 - [15] All kinematic quantities presented in this paper are evaluated in the rest frame of the initial e^+e^- system.
 - [16] M. Ablikim *et al.*, BESIII Collaboration, Measurement of the absolute branching fraction of $D^+ \rightarrow \bar{K}^0 e^+ \nu_e$ via $\bar{K}^0 \rightarrow \pi^0 \pi^0$, Chin. Phys. C **40** (2016) 113001, <http://dx.doi.org/10.1088/1674-1137/40/11/113001>, arXiv:1605.00208.
 - [17] M. Ablikim, et al., BESIII Collaboration, Measurements of Absolute Hadronic Branching Fractions of the Λ_c^+ Baryon, Phys. Rev. Lett. **116** (2016) 052001, <https://doi.org/10.1103/PhysRevLett.116.052001>, arXiv:1511.08380.
 - [18] P. L. Frabetti *et al.*, E687 Collaboration, First observation of the $\Sigma^- \pi^+ \pi^+$ decay mode of the Λ_c baryon and its branching ratio relative to the $\Sigma^+ \pi^+ \pi^-$ mode, Phys. Lett. B **328** (1994) 193, [http://dx.doi.org/10.1016/0370-2693\(94\)90450-2](http://dx.doi.org/10.1016/0370-2693(94)90450-2).